ISSN: 1813-162X (Print) ; 2312-7589 (Online)

Tikrit Journal of Engineering Sciences

available online at: http://www.tj-es.com

Efficient T-OOFDM System to Mitigate the Dispersion of Long-Haul Optical Fiber Channel at WANs

Mohammed Shweesh Ahmed *

Petroleum System Control Engineering Department
College of Petroleum and Minerals Engineering
Tikrit University
Salahaldeen
Iraq

***Keywords*:**

Orthogonal frequency division multiplexing (OFDM)
T-transform
bit error rate (BER)
iber optics
theoretical analysis

ARTICLE INFO

Article history:

Received 17 October 2017
Accepted 20 December 2017
Available online 01 September 2018

ABSTRACT

Due to its attractive features, the utilization of fiber optics as a transmission medium with various applications is increased rapidly. In despite, when signals are transmitted with high data rates through ultra-long haul distances of single-mode fiber (SMF), which is usually used at wide area networks (WANs), the nonlinear dispersion of signals is raised. This phenomenon leads digital pulses to interfere with the adjacent pulses. In this paper, an optical orthogonal frequency division multiplexing based T-transform (T-OOFDM) system is proposed to mitigate the effect of fiber dispersion significantly and reduce the peak-to-average power ratio (PAPR) of the transmitted signal when compared with conventional optical OFDM (OOFDM) system. Simulations results confirmed by the analytical analysis demonstrated that the detrimental effects arising from fiber channel dispersion on the subcarrier orthogonality of the transmitted signals can be efficiently minimized by using T-OOFDM system. Moreover, the peak of the transmitted signal will be considerably reduced whilst preserving the average power of signals.

DOI: http://dx.doi.org/10.25130/tjes.25.3.02

نظام T-OOFDM الكفوء لمعالجة التشتت في قنوات الخلايا الضوئية في شبكات المساحات

الخلاصة

نظرا لخصائصها الجذابة، توظيف الخلايا الضوئية كوسط ارسال مع مختلف التطبيقات ازداد بسرعة. مع ذلك، عندما تنتقل الاشارات بمعدل عالي ولمسافات بعيدة بواسطة خلايا النمط المفرد (SMF)، والتي هي عادة تستخدم في شبكات المساحات الشاسعة (WAN)، فان مشكلة التشتت الغير خطي تزداد. هذه الظاهرة تجعل الاشارات الرقمية تتداخل مع الاشارات المجاورة. في هذا العمل، نظام اختيار الترددات المتعامدة المقسمة باستخدام الخلايا الضوئية (T-OOFDM) اقترح لمجابهة نتيجة تاثير التشتت الضوئي وبأثر واضح كذلك لتقليل نسبة القمة على المعدل لطاقة الاشارة المرسلة بالمقارنة مع نظام (OOFDM) التقليدي. النتائج المؤكدة والمدعومة بواسطة التحليل النظري تبين ان تشتت الضوء في قنوات الخلايا الضوئية وتأثيرها الضار على تعامد حوامل الاشارة المرسلة يمكن ان يقلل وبكفاءة باستخدام نظام T-OOFDM. علاوة على ذلك، قمة طاقة الاشارة المرسلة سوف تقلل وبوضوح مع عدم التاثير على معدل طاقة الاشارات المرسلة.

1. INTRODUCTION

High bandwidth, helpful size, low noise power, low power consumption and low attenuation, are the main features of optical fiber. Consequently, it has been utilized widely during the last few decades as an efficient transmission medium to connect networks of the whole world [1]. Depending on the characteristics and applications, fiber optics can be classified into two types; Single mode fiber (SMF) and multi-mode fiber (MMF). SMF is typically used with the long-haul systems, which are the wide area networks (WANs). The dominant linear impairments in such a type are group-velocity dispersion (GVD), which means different frequencies travel at different speeds, and polarization-mode dispersion (PMD), which means different polarizations arrive at the receiver with different delays [2].

Although there are many advantages of fiber optics, but dispersion and nonlinearity, which occur as consequences of transmitting high bit rate data by using narrow optical pulses, represent main challenges of fiber

* *Corresponding author: E-mail* : mohammed.shwash@tu.edu.iq

optics utilization with networks. Through long haul distances, the dispersion of light pulses leads inter-symbol interference (ISI) between adjacent pulses to be occurring. As a result, a lot of transmitted data bits will be lost, which leads to reduce the efficiency of systems that using fiber-optics as transmission media. Therefore, these issues are received a great attention in the recent studies.

Single-carrier modulation with digital equalization is efficiently used with different optical applications [3]. However, with the advances in digital receivers for optical systems, and due to its attractive features, orthogonal frequency division multiplexing (OFDM) can be employed efficiently to mitigate the negative ramifications of fiber optic dispersion [4]. Thus, owing to its robustness against ISI, since the symbol period of each subcarrier can be made long compared to the delay spread caused by GVD and PMD, OFDM has been received a great interest in the fiber-optic research community [5,6]. The spectral efficiency of OFDM increases the robustness of such a system, which is measured against the dispersion of fiber optic channel [7]. Despite this, it is noteworthy that the overall OFDM signal spectrum fades selectively; consequently, certain subcarriers will be attenuated by deep fades. In such cases, OFDM does not offer any improvement in performance since no diversity is exploited to recover the attenuated subcarriers. Furthermore, the coherent superposition of a large number of subcarriers through the IFFT may produce samples with very high peak values with respect to its average symbol power [8]. Therefore, various schemes have been devised to eliminate such deleterious effects, although with high complexity, data rate losses and BER performance degradation.

In this work, an optical OFDM based T-transform (T-OOFDM) system is used instead of the conventional optical OFDM (OOFDM) system. Due to its ability to increase the diversity of the transmitted signals, T-OOFDM system achieves an outstanding BER mprovement when compared with the conventional OOFDM system over long haul distances of SMF, which is usually used at WANs. Furthermore, due to the low superposition of the subcarriers passing through the T-transform, T-OOFDM achieves a noticeable PAPR reduction as a consequence of reducing the high peak of the transmitted signal through the fiber optics whilst preserving the average transmitted power and data rate.

The rest of this paper is organized as follows. Section II briefly presents the optical networks. The inverse T-transform is introduced in Section III. Section IV describes the mathematical model of the proposed T-OOFDM scheme. Mathematical analysis of the BER performance for the T-OOFDM system is presented in Section V. Section VI presents the simulation results, along with their discussion. Lastly, Section VII concludes the paper.

2. OPTICAL NETWORKS

Based on the coverage area, the main classes of optical networks are: Personal area networks (PANs), local area networks (LANs), metropolitan area networks (MANs) and WANs, where the basic attributes of these Networks can be summarized as in Table 1.

WANs, which are considered as long-haul systems, typically use SMF. The main impairments of such a mode are GVD and PMD. To overcome the negative influence of such two phenomena, coherent detection scheme, which means detection of phase and amplitude of the optical electric field, is utilized with WANs [2]. In addition, amplified spontaneous emission (ASE), which is considered as the dominant noise over thermal and shot noises, is modeled as a complex additive white Gaussian noise (AWGN). Due to the optical amplifier, the optical system nonlinearity is increased and its performance is degraded as a consequence of ASE [9].

Table 1
Some characteristics of different optical networks.

Applications	PAN (10m)	LAN (0.35km)	MAN (50-500km)	WAN (>1000km)
Bit rate	300 Mbit/s	10-100 Gbit/s	10-100 Gbit/s	100-1000 Gbit/s
Medium	Free space	MMF	SMF	SMF
Dominant Dispersion	Multipath (Linear)	Multimode (Linear)	Chromatic (Nonlinear)	Chromatic/Polar. (Nonlinear)
Dominant Noise	Ambient light (Shot noise)	Thermal (AWGN)	Amplifier (Chi-square)	Amplifier (AWGN)
Other effects	Clipping noise	Clipping noise	Clipping noise	Fiber nonlinearity

Moreover, SMF is also used with MANs, but the direct detection scheme is utilized at the receiver side. However, at the transmitter of MANs, either electric field or power intensity can be modulated. Therefore, due to the nonlinear photo detection process, the ASE noise is no longer Gaussian and becomes Chi-square distributed. Thus, the detection process becomes more complicated as a consequence of the interaction between the ASE and the received signal at the receiver side of MANs [10]. On the other hand, LANs typically use MMF. In a sequel, different propagation modes utilize intensity modulation with direct detection schemes without considering the ASE. Whereas, the dominant noises that should be taken into account are thermal noise or shot noise from the receiver [11]. Finally, air or free space is utilized as a transmission medium with the PANs. Therefore, multipath propagation is the main impairment of optical wireless systems that are used in short distance applications. Consequently, the negative ramification of arriving different reflections of signal with different delays at the receiver side is compensated for by using intensity modulation with direct detection. Similar to LANs, the dominant noises are the thermal and ambient light (shot) noises.

3. INVERSE T-TRANSFORM STRUCTURE WITH SIZE N = 32

Forward T-transform with 16-points was reported in [12-14]. In contrast, this work introduces the inverse T-transform with 32-points. For simplicity purpose, same steps in [12] are followed. Thus, size N inverse T-transform, $\hat{T}^H$, can be expressed as,

$$\hat{T}^H = \frac{1}{N} W \hat{F}^H \tag{1}$$

where W and $\hat{F}^H$ are the normalized $N \times N$ WHT matrix and the IFFT matrix rearranged by column reversed order, respectively. In order to avoid redundancy W and $\hat{F}^H$ are simplified in [12]. Consequently, by following the same approach in [12], and after factorizing W and $\hat{F}^H$, for the case of N = 32, Eq. (1) can be written as,

$$\hat{T}_{32} = \frac{1}{32}\begin{bmatrix} 2W_{16}\hat{A}_{16} & 0 \\ 0 & 2W_{16}\hat{B}_{16} \end{bmatrix} \tag{2}$$

$\hat{A}$ and $\hat{B}$ can be simplified more as in Eq. (3), where $\hat{Y}$ and $\hat{\theta}$ are the sub-matrices of $\hat{A}$, $\hat{\beta}$ and $\hat{\xi}$ are the sub-matrices of $\hat{B}$ that can be factorized more as in Eq. (4). $\hat{\alpha}, \hat{\delta}, \hat{\zeta}, \hat{\eta}, \hat{\lambda}, \hat{\nu}, \hat{\varphi},$ and $\hat{\rho}$ are the sub-matrices of the rearranged IFFT matrix, $\hat{F}^H$.

Ultimately, after calculating the elements of sub-matrices in Eq. (4), the flowchart of T-transform for N = 32 can be represented as shown in Fig. 1, where X_{th} stands for Walsh-domain samples, x_{th} stands for time-domain samples, $a^n = (1 - w^n)/2$, and $w = e^{j2\pi/N}$.

The structure of every single butterfly along with complexity calculations are briefly explained in [12].

(3)

$$\hat{T}_{32} = \frac{1}{32}\begin{bmatrix} 4W_8\hat{Y}_8 & 0 & 0 & 0 & 0 & 0 \\ 0 & 4W_8\hat{\theta}_8 & 0 & 0 & 0 & 0 \\ & & 2W_8\hat{\beta}_8(1+w^8) & 2W_8\hat{\xi}_8(1-w^8) \\ & & 2W_8\hat{\beta}_8(1-w^8) & 2W_8\hat{\xi}_8(1+w^8) \end{bmatrix}$$

(4)

$$\hat{T}_{32} = \begin{bmatrix} 8W_4\hat{\alpha}_4 & 0 & 0 & 0 & 0 & 0 \\ 0 & 8W_8\hat{\delta}_4 & 0 & 0 & 0 & 0 \\ 0 & 0 & 4(1+w^8)W_4\hat{\zeta}_4 & 4(1-w^8)W_4\hat{\eta}_4 \\ 0 & 0 & 4(1-w^8)W_4\hat{\zeta}_4 & 4(1+w^8)W_4\hat{\eta}_4 \\ & & 2(1+w^8)(1+w^4)W_4\hat{\lambda}_4 & 2(1+w^8)(1-w^4)W_4\hat{\nu}_4 & 2(1-w^8)(1+w^{12})W_4\hat{\varphi}_4 & 2(1-w^8)(1-w^{12})W_4\hat{\rho}_4 \\ & & 2(1+w^8)(1-w^4)W_4\hat{\lambda}_4 & 2(1+w^8)(1+w^4)W_4\hat{\nu}_4 & 2(1-w^8)(1-w^{12})W_4\hat{\varphi}_4 & 2(1-w^8)(1+w^{12})W_4\hat{\rho}_4 \\ & & 2(1-w^8)(1+w^4)W_4\hat{\lambda}_4 & 2(1-w^8)(1-w^4)W_4\hat{\nu}_4 & 2(1+w^8)(1+w^{12})W_4\hat{\varphi}_4 & 2(1+w^8)(1-w^{12})W_4\hat{\rho}_4 \\ & & 2(1-w^8)(1-w^4)W_4\hat{\lambda}_4 & 2(1-w^8)(1+w^4)W_4\hat{\nu}_4 & 2(1+w^8)(1-w^{12})W_4\hat{\varphi}_4 & 2(1+w^8)(1+w^{12})W_4\hat{\rho}_4 \end{bmatrix}$$

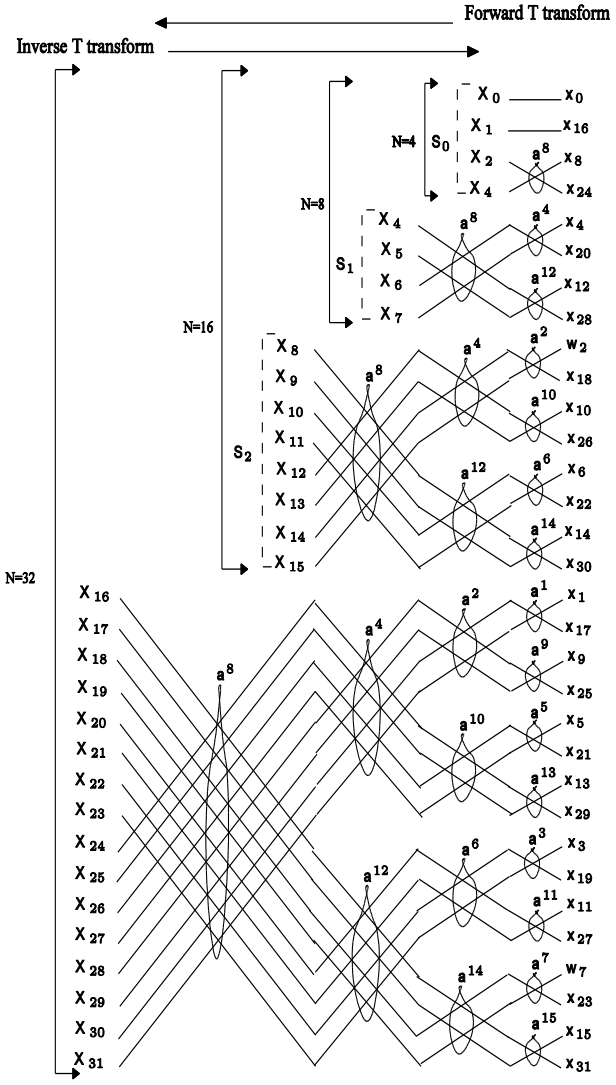

Fig. 1. T-transform flowchart with N = 32.

4. MATHEMATICAL DESCRIPTION OF T-OOFDM SYSTEM

The time-domain samples are generated by applying the modulated data vector $X = [X_0,\ X_1, \dots ,\ X_{N-1}]^{\ T}$ to N-points inverse T-transform,

$$x = \hat{T}^H X \tag{5}$$

where $x = [x_0,\ x_1, \dots ,\ x_{N-1}]$, $\hat{\mathbf{T}}$ is the $N\times N$ inverse T-transform unitary matrix, which was illustrated on the previous section, and $(.)^H$denotes the Hermitian operator. Thus, Eq. (5) can be rewritten as,

$$x = W\hat{F}^H X \tag{6}$$

$$x = \hat{F}^H \hat{X} \tag{7}$$

where $\hat{X} = WX$ is the frequency-domain samples of Walsh-domain samples X.

A time-domain guard band is created by appending the last N_g samples of x as a preamble for the samples $x_0, x_1, \dots, x_{N-1}$. In order to prevent ISI, the length of cyclic prefix (CP) should be greater than the maximum delay spread of the channel.

At the receiver side, for more simplicity of analysis, the T-transform will be subdivided into its original transforms. Thus, the received frequency-domain samples, after removing the CP samples in time-domain, can be expressed as,

$$s = Fr = D_H \hat{X} + Z \tag{8}$$

where r is the received time-domain samples, Z is the FFT of the Gaussian noise vector, and D is the channel matrix. Because the channel matrix is circulant, it can be diagonalized in frequency-domain with k-th diagonal element as, $(k) = \sum_{l=0}^{L} h(l) e^{-\frac{j2\pi kl}{N}}$, h and L represent channel taps in time-domain, and the channel path number, respectively.

In order to eliminate the effects of channel, the received signal should be equalized either in Walsh-domain or in frequency-domain. As it can be noted from Eq. (8), this can be achieved if the matrix D_H; or an estimated version of $D_H(\widehat{D}_H)$ is available. However, in frequency-domain, multiplying the FFT output by D_H^{-1} also affects the noise; consequently we use the minimum mean square error (MMSE) equalizer to minimize the noise enhancement. Therefore, the k-th equalized sample can be computed as,

$$\acute{X}_k = €_k s_k = €_k D_{k,k} \hat{X}_k + €_k Z_k \tag{9}$$

where $€_k$ is the MMSE coefficient at the k-th subcarrier,

$$€_k = \frac{\widehat{D}^*_{k,k}}{\left|\widehat{D}_{k,k}\right|^2 + \frac{1}{\Gamma_k}} \tag{10}$$

where $\Gamma_k$is the signal-to-noise ratio (SNR) of k-th subcarrier.

As a result, the received equalized signal, X'' in Walsh-domain can be computed as,

$$X'' = W\,X', = \underbrace{W€D\hat{X}}_{\Omega} + W€Z \tag{11}$$

5. PERFORMANCE ANALYSIS

In order to verify the simulation results, this section illustrates the performance analysis of the T-OOFDM system across the fiber-optic channels. Performance analysis is achieved with the assumption that the input symbols are uncorrelated with the same variance E_s in real and imaginary parts. Also, the noise is assumed to be independent white Gaussian noise with variance N_0.

Basically, the performance of OFDM system with M-PSK and M-QAM modulations over a white complex Gaussian noise channel can be expressed as,

$$P_{e_{\mathrm{M-PSK-OFDM}}} = \frac{\varepsilon}{m} Q\left(\sqrt{2\Gamma}\,\sin(\pi/M)\right), \tag{12}$$

$$P_{e_{\mathrm{M-QAM-OFDM}}} = \frac{(4 - 2^{(2-M/2)})}{m} Q\left(\sqrt{2\Gamma/(M-1)}\right), \tag{13}$$

where ϵ stands for the average number of nearest neighbors signal points, $m = \log_2(M)$ is the number of bits in each constellation sample, Γ is the signal-to-noise ratio (SNR) E_s/N_0, $E_s$is the power per symbol, N_0stands for the Gaussian noise average power, and $Q(x) = \frac{1}{\sqrt{2\pi}} \int_x^\infty e^{-t^2/2}\, dt$.

In a sequel, the performance analysis of any system over any transmission media essentially depends on the calculation of the new values of SNR that appear in

Eq. (12) and Eq. (13) which take the effect of transmission media into account [12]. Consequently, the general form of the average SNR for the T-OOFDM system's received signal, which shown in Eq. (11), can be expressed as,

$$\Gamma_{\mathrm{T-OOFDM}} = \frac{E|\Omega|^2}{E|X''|^2 - E|\Omega|^2} \tag{14}$$

Parts of Eq. (14) can be recalculated with MMSE criterion. Due to orthogonality of *W* and *F*,

$$E|\Omega|^2 = E_s \frac{1}{N}\left(\sum_{k=0}^{N-1} \frac{\left|\widehat{D}_{k,k}\right|^2}{\left|\widehat{D}_{k,k}\right|^2 + \frac{1}{\Gamma_k}}\right) \tag{15}$$

Also, the noise variance can be computed as in Eq. (16). Upon substituting Eq. (15) and Eq. (16) into Eq. (14), we get

$$|X''|^2 - E|\Omega|^2 = E_s\left[\sum_{k=0}^{N-1} \frac{\left|\widehat{D}_{k,k}\right|^2}{\left|\widehat{D}_{k,k}\right|^2 + \frac{1}{\Gamma_k}}\left(1 - \frac{1}{N}\sum_{k=0}^{N-1} \frac{\left|\widehat{D}_{k,k}\right|^2}{\left|\widehat{D}_{k,k}\right|^2 + \frac{1}{\Gamma_k}}\right)\right] \tag{16}$$

$$\Gamma_{\mathrm{T-OOFDM}} = \frac{\frac{1}{N}\left(\sum_{k=0}^{N-1} \frac{\left|\widehat{D}_{k,k}\right|^2}{\left|\widehat{D}_{k,k}\right|^2 + \frac{1}{\Gamma_k}}\right)}{\left[1 - \frac{1}{N}\left(\sum_{k=0}^{N-1} \frac{\left|\widehat{D}_{k,k}\right|^2}{\left|\widehat{D}_{k,k}\right|^2 + \frac{1}{\Gamma_k}}\right)\right]} \tag{17}$$

Mathematically, it can be proven that,

$$N\left[1 - \frac{1}{N}\left(\sum_{k=0}^{N-1} \frac{\left|\widehat{D}_{k,k}\right|^2}{\left|\widehat{D}_{k,k}\right|^2 + \frac{1}{\Gamma_k}}\right)\right] = \sum_{k=0}^{N-1} \frac{1}{\left|\widehat{D}_{k,k}\right|^2 + \frac{1}{\Gamma_k}} \tag{18}$$

In the sequel,

$$\Gamma_{\mathrm{T-OOFDM}} = \frac{\left(\sum_{k=0}^{N-1} \frac{\left|\widehat{D}_{k,k}\right|^2}{\left|\widehat{D}_{k,k}\right|^2 + \frac{1}{\Gamma_k}}\right)}{\left(\sum_{k=0}^{N-1} \frac{1}{\left|\widehat{D}_{k,k}\right|^2 + \frac{1}{\Gamma_k}}\right)} \tag{19}$$

Eventually, the BER performance of T-OOFDM over a fiber-optic channel, which fixed within the entire period of T-OOFDM symbol transmission with QPSK and 16-QAM, can be evaluated by substituting Eq. (19) into Eq. (12) and Eq. (13), respectively.

6. SIMULATION RESULTS AND DISCUSSION

Without loss of generality, presented results in this section are obtained based on assumptions of perfect knowledge of channel response, and perfect frequency and time synchronization. On the other hand, as a consequence of reducing the superposition of the subcarriers passed through the inverse T-transform at the transmitter side, which leads to reduce the peak of the transmitted signals, the PAPR of the T-OOFDM scheme will be lower than that of OOFDM system. Due to the unitary characteristics of the T-transform, peak reduction is achieved with the preservation of average power for the transmitted samples. PAPR reduction of T-OFDM system was presented in [12]. So, it will be omitted in this w ork.

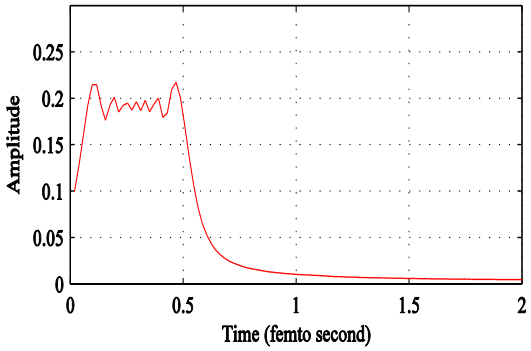

Fig. 2. Channel type I.

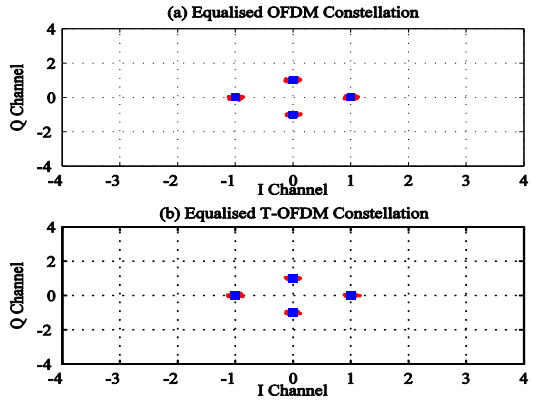

Fig. 3. Constellations of T-OFDM and OFDM systems over fiber optic channel I, SNR = 25 and QPSK.

BER is a typical performance measure for quantifying the benefits of using the proposed T-OOFDM system over the conventional OOFDM system. In order to investigate the BER performance of such systems over SMF, we have evaluated the performance of such systems based on the following parameters: the subcarriers number is 1024, the

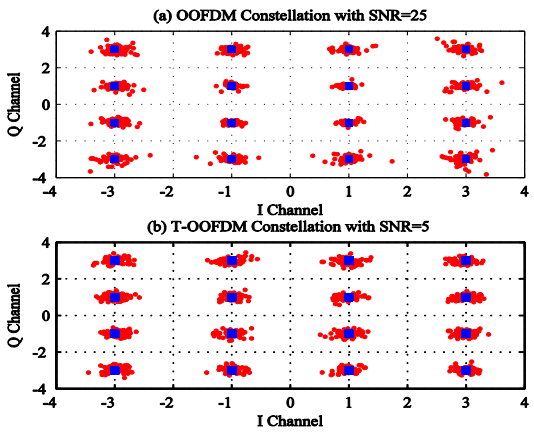

Fig. 4. Constellations of T-OFDM and FDM systems over fiber optic channel I, SNR = 25 and 16-QAM.

CP length is 256, light velocity (c) = 3×10^8, dispersion = 17 ps/(nm km), channel length = 80 km. It should be noted that the quasi-static (fixed within entire T-OOFDM symbol transmission period) two types SMF channels (channel I and channel II shown in Figs. 2 and 6, respectively) are adopted to evaluate the BER performance of the proposed system. As a consequence, for its ability to increase the diversity of transmitted signals, T-OOFDM system achieves a noticeable BER performance improvement compared with the conventional OOFDM system when measured over slow fading of channel I, as clearly shown in Fig. 5. On the other hand, as clearly known in the literature, the main challenge of the conventional OOFDM system is the severe fading, channel II. Interestingly, the diversity of T-OOFDM system, when using with MMSE equalizer, mitigates the deleterious effect of channel II on the transmitted samples and leads to achieve an outstanding performance over such a type of channel, as clearly shown in Fig. 9. In addition, in order to determine the effective value of SNR for each system, the constellations of the transmitted samples with various SNR values are illustrated in Figs. 3, 4, 7, and 8.

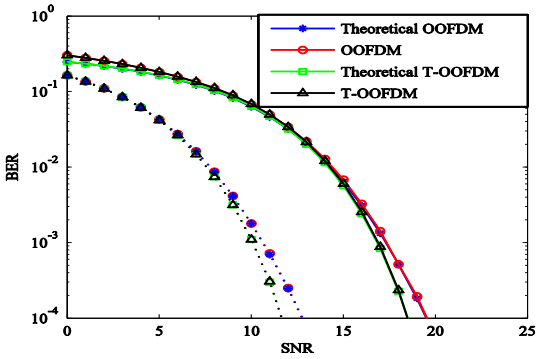

Fig. 5. BER performance of T-OOFDM, conventional OOFDM systems with channel I, QPSK (Dash lines) and 16-QAM.

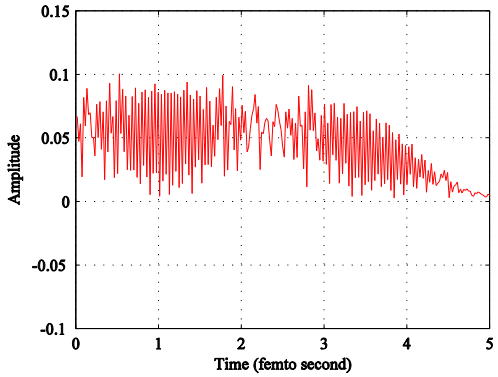

Fig. 6. Channel type II.

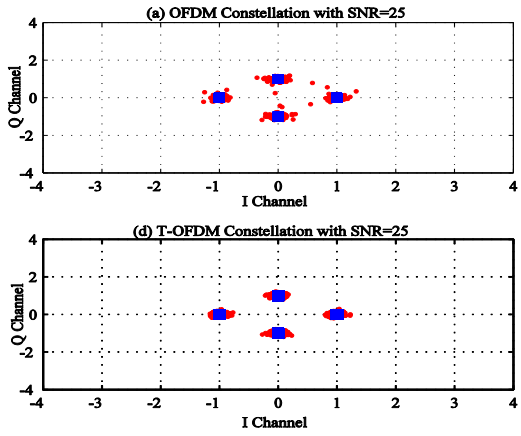

Fig. 7. Constellations of T-OFDM and OFDM systems over fiber optic channel II, SNR=25 and QPSK.

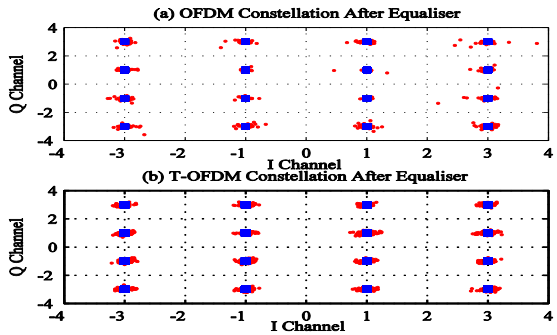

Fig. 8. Constellations of T-OFDM and OFDM systems over fiber optic channel II, SNR=35 and 16-QAM.

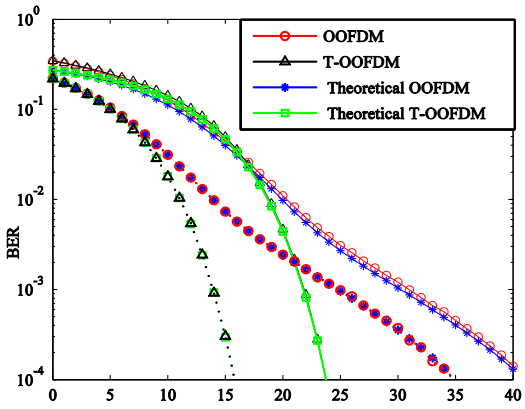

Fig. 9. BER performance of T-OFDM, conventional OFDM systems with channel II, QPSK and 16-QAM.

7. CONCLUSIONS

In this work, an efficient transmission technique, T-OOFDM, is proposed to reduce the nonlinear dispersion that is raised when signals are transmitted with high data rates through ultra-long haul distances of single-mode fiber (SMF), which is usually used at wide area networks (WANs). As it demonstrated in the simulation results, which is analytically supported, the spreading of each subcarrier over others introduces frequency diversity for the transmitted samples which leads to reduce the effect of deep fading channels. Consequently, the T-OOFDM system achieves a significant improvement in the BER performance across the long-haul fiber-optics channel.

REFERENCES

[1] Agrawal GP. Fiber-optic communications systems. 3rd ed. USA: John Wiley & Sons Inc.; 2002.

[2] Shieh W. PMD-supported coherent optical OFDM systems. *IEEE Photonics Technology Letters* 2007; **19** (3): 134-136.

[3] Zhu C, Tran A, Do C. Digital signal processing for training-aided coherent optical single-carrier frequency-domain equalization systems. *Journal of Lightwave Technology* 2014; **32** (24): 4712-4722.

[4] Moreolo MS, Muoz R, Junyent G. Novel power efficient optical OFDM based on Hartley transform for intensity-modulated direct-detection systems. *Journal of Lightwave Technology* 2010; **28** (5): 798-805.

[5] Jansen SL, Morita I, Takeda N, Tanaka H. 20-Gb/s OFDM transmission over 4160 km SSMF enabled by RF-pilot tone phase noise compensation. *Optical Fiber Communication Conference and Exposition and The National Fiber Optic Engineers Conference.* 2007, March 25-29; California, USA; pp. 9-16.

[6] Tang JM, Shore KA. 30-Gb/s transmission over 40-km directly modulated DFB-laser-based single-mode-fiber links without optical amplification and dispersion compensation. *Journal of Lightwave Technology* 2006; **24** (6): 2318-2327.

[7] Andrews JG, Ghosh A, Muhamed R. Fundamentals of WiMAX, understanding broadband wireless networking. USA: Prentice Hall; 2007.

[8] Hanzo L, Munster M, Choi BJ, Keller T. OFDM and MC-CDMA for broadband multiuser communic-ations WLANs and broadcasting. USA: John Wiley & Sons Inc.; 2003.

[9] Ibrahim SK, Zhao J, Rafique D, Dowd J, Ellis AD. Demonstration of "world-first experimental optical fast OFDM system at 7.174 Gbit/s and 14.348 Gbit/s. *36th European Conference and Exhibition on Optical Communication*. 2010, September 19-23; Torino, Italy.

[10] Lei C, Chen H, Chen M, Xie S. A 10 Gb/s DFT based fast optical OFDM scheme with double spectral efficiency. *CLEO-Laser Science to Photonic Applications.* 2011, May 1-6; Baltimore, MD, USA.

[11] Giacoumidis E, Tomkos I, Tang JM. A performance of optical fast-OFDM in MMF-based links. *Optical Fiber Communication Conference and Exposition and the National Fiber Optic Engineers Conference*. 2011, March 6-10; Los Angeles, USA; pp.17.23.

[12] Ahmed MS, Boussakta S, Sharif B, Tsimenidis CC. OFDM based on low complexity transform to increase multipath resilience and reduce PAPR. *IEEE Transaction on Signal Processing* 2011; **59** (12): 5994-6007.

[13] [13] Ahmed MS, Boussakta S, Sharif B, Tsimenidis CC. OFDM based new transform with BER performance improvement across multipath transmission. *IEEE International Conference on Communication*. 2010, May 23-27; Cape Town, South Africa; pp. 1-5.

[14] Boussakta S, Holt AG. Fast algorithm for calculation of both Walsh-Hadamard and Fourier transforms (FWFTs). *IEE Electronics Letters* 1989; **25** (20):1352-1354.